DYNAMIC INJURY TOLERANCES FOR LONG BONES OF THE FEMALE UPPER EXTREMITY

S. Duma[1], P. Schreiber[1], J. McMaster[1,2], J. Crandall[1], C. Bass[1], and W. Pilkey[1]
1. Automobile Safety Laboratory, University of Virginia
2. Department of Orthopaedics, University of Nottingham

ABSTRACT

This paper presents the dynamic injury tolerances for the female humerus and forearm derived from dynamic three-point bending tests using 22 female cadaver upper extremities. Twelve female humeri were tested at an average strain rate of 3.7 ± 1.3 strain/second. The strain rates were chosen to be representative of those observed during upper extremity interaction with frontal and side airbags. The average moment to failure when mass scaled for the 5th% female was 128 ± 19 Nm. Using data from the in-situ strain gages during the drop tests and geometrical properties obtained from pre-test CT scans, an average dynamic elastic modulus for the female humerus was found to be 24.4 ± 3.9 GPa. The injury tolerance for the forearm was determined from 10 female forearms tested at an average strain rate of 3.94 ± 2.0 strain/second. Using three matched forearm pairs, it was determined that the forearm is 21% stronger in the supinated position, 91 ± 5 Nm, versus the pronated position, 75 ± 7. Two distinct fracture patterns were seen for the pronated and supinated groups. To produce a conservative injury criterion, a total of 7 female forearms were tested in the pronated position, which resulted in the forearm injury criterion of 58 ± 12 Nm when scaled for the 5th% female. It is anticipated that this data will provide injury reference values for the female forearm during driver air bag loading, and the female humerus during side air bag loading.

INTRODUCTION

Although air bags have reduced the risk of fatal injuries in automobile collisions, they have increased the incidence of nonfatal injuries including upper extremity injuries. It is suggested that there may be a 40% increase in risk of serious (AIS 3) upper extremity injury to belted occupants with air bags versus those without air bags [NHTSA, 1996]. Kuppa *et al.* showed that 1.1% of drivers who were restrained by only a seat belt experienced an upper extremity injury, versus 4.4% of drivers in the presence of a deploying air bag who experienced an upper extremity injury [Kuppa *et al.*, 1997]. Although air bag depowering is expected to have a beneficial effect on the rate of upper

extremity injuries from air bags, the injury tolerances of the humerus and forearm must be known in order to design driver and side air bags that minimize the risk of serious injury to the upper extremities.

Given that in general female bones have a lower mineral content and are thus weaker than male bones, the injury tolerance for small females provides a conservative estimate for the general driving population. Several papers have addressed the humerus bending strength and the results are summarized in Table 1. All previous experiments were performed under quasistatic conditions. It has been shown that the strength of bone increases with increased strain rate [Carter, 1983]. This indicates that the previous studies underestimate the strength of bone in a dynamic environment. Moreover, the studies by Weber (1859) and Messerer (1880) are dated and involve sample populations that are likely different than the modern population. Kallieris *et al.* (1997) performed tests involving only males, while Kirkish *et al.* (1996) tested only one female. The current study addresses the lack of recent, dynamic tests with female humeri.

Table 1: Published Humerus Tolerance Data

		Male	Female
Study	**Year**	**Bending Failure (Nm)**	**Bending Failure (Nm)**
Weber	1859	115	73
Messerer	1880	151	85
Kirkish	1996	155 (± 45)	84
	scaled	230 (50^{th}%)	134 (5^{th}%)
Kallieris	1997	138 (± 9)	

The risk of injury to the forearm from the driver side air bag has been investigated. Bass *et al.* (1997) compared air bag tests with cadaveric upper extremities with matched tests using the SAE fully instrumented 5^{th}% female upper extremity. They found that a forearm moment of 67 Nm in the dummy corresponded to a 50% risk of at least one fracture in the radius and ulna. However, no direct dynamic bending moment tests on female forearms were done in that study. Furthermore, while quasistatic tests have been performed on the radius and ulna separately, no published dynamic tolerance data exists for the intact female forearm. An additional goal of the forearm test series was to determine the difference in dynamic bending strength between supinated and pronated forearms. In the supinated position, the radius and ulna are essentially parallel to each other, where as in the pronated position, the distal radius rotates over the ulna and brings the radius above and across the ulna. The purpose of this study was to determine the dynamic bending strengths of the female humerus and forearm, and to investigate the relationship between forearm strength and radius and ulna orientation.

METHODOLOGY

HUMERUS TESTS -- Twelve female humeri were prepared by disarticulating the upper extremity at the shoulder and elbow joints. As shown

in the Appendix Table A1, the average age of these specimens was 57 ± 11 years with an average body mass of 58.7 ± 7.6 kg. Enough soft tissue was removed from each humerus to expose 50 mm of bone at the distal and proximal ends. The exposed ends were potted in PC-7 epoxy putty to a depth of 30 mm using removable molds. Simple support fixtures were attached to the hardened epoxy as shown in Figure 1. Strain gages (Micro Measurements, model CAE-13-125UN-350) were adhered mid-shaft on both the anterior and posterior sides of the humerus to provided maximum tensile and compressive strains. Pre-test CT scans of each humerus were taken (5 mm contiguous slices) to determine bone cross-sectional properties. Pre-test radiographs (frontal and sagittal views) were taken to identify and pre-existing skeletal conditions. If any abnormal bone pathology was noticed, the specimen was removed from the test population. Post-test radiographs (frontal and sagittal views) were taken and the humerus dissected to evaluate induced injury and classify fracture patterns.

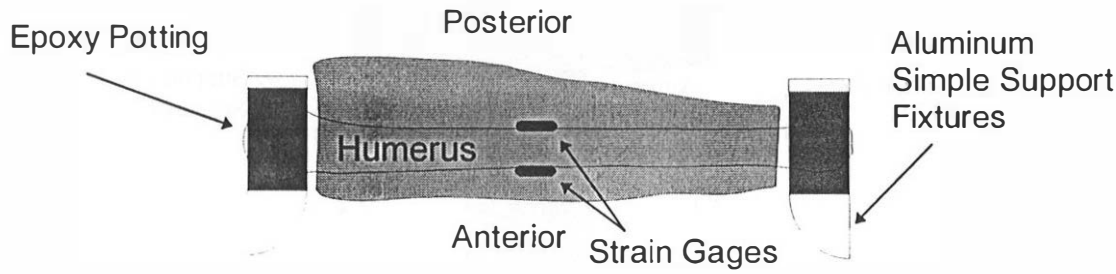

Figure 1: Humerus Preparation and Instrumentation

Dynamic three-point bending tests were performed using a 9.48 kg impactor released from a drop height of 1.35 m. The impactor was guided by a vertical linear bearing track which resulted in a pre-impact velocity of 3.63 m/s. This velocity was chosen to match humerus strain rates as measured in cadaveric subjects under side air bag loading. The humerus was impacted mid-shaft in the posterior-anterior direction as shown in Figure 2. This direction was chosen to correspond with the direction of humerus loading that would be seen from a deploying seat mounted side air bag. The impactor was brought to rest following fracture using a soft stop decelerator of crushable polystyrene. The proximal and distal simple supports each rested on greased plates. Each plate was supported by three quartz piezoelectric load sensors (PCB Piezotronics, model P212-B) aligned to measure force in the vertical direction. The impactor load was measured using three piezoelectric load sensors mounted in a similar fashion between the impactor blade and impactor mass. Accelerometers mounted to the impactor blade allowed for inertial compensation of the impact load. The initial contact between the impactor and the humerus was recorded by placing a conductive trigger switch on the humerus. Data was sampled at a rate of 20,000 Hz, and filtered at SAE class 1000. High speed video (Kodak, model 1000-E, 1000 fps) recorded impactor displacement during the event.

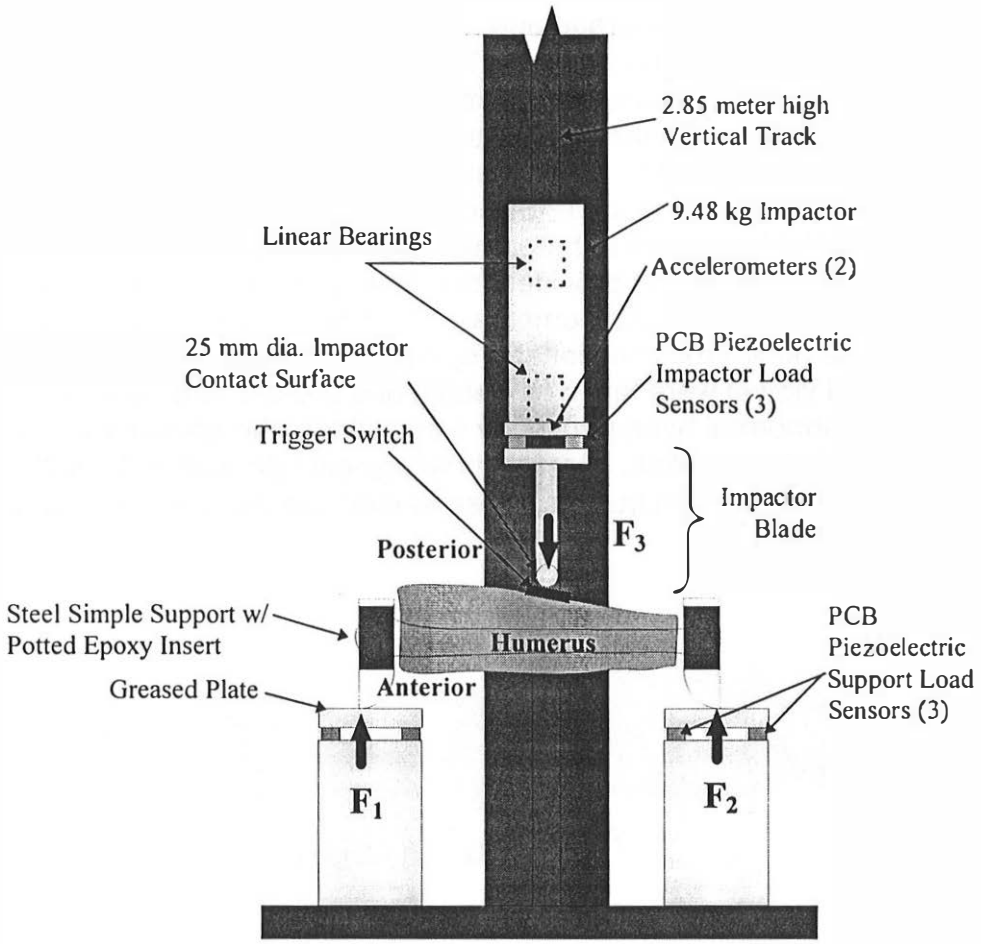

Figure 2: Drop Test Configuration for the Humerus Tests

FOREARM TESTS -- Ten female forearms were prepared by disarticulating the upper extremity at the shoulder and keeping the elbow joint intact. As shown in the Appendix Table A2, the average age of these specimens was 61 ± 5 years with an average body mass of 59.1 ± 11.6 kg. Simple mounts were designed to attach to the posterior side of the forearm via two tie wraps as shown in Figure 3. This mounting technique allowed for the forearm to be oriented in the supinated or pronated position prior to testing. The three-point drop test device used for the humerus tests was again employed with the drop height adjusted to 2.0 m resulting in an impact velocity of 4.42 m/s. This velocity was chosen to match radius and ulna strain rates as measured in cadaveric tests with driver side air bags [Bass, 1997]. In both the pronated and supinated positions, the upper extremity was positioned such that the impactor struck the anterior surface of the forearm. The impact location was established as the distal third of the forearm, which was taken as two-thirds of the ulna length measured distally from the olecranon. This location was chosen due to the local minimum polar moment of inertia of both the ulna and radius at the distal third of the forearm [Bass, 1997]. Due to the lack of bone symmetry in the ulna and radius, strain gage rosettes (Micro Measurements, model CAE-06-062UR-350) where used so that the principle strains could be determined. One rosette was placed at the distal third mark on both the

posterior radius and posterior ulna. The two tailed Students t-test with alpha = .05 was used to compare the data averages.

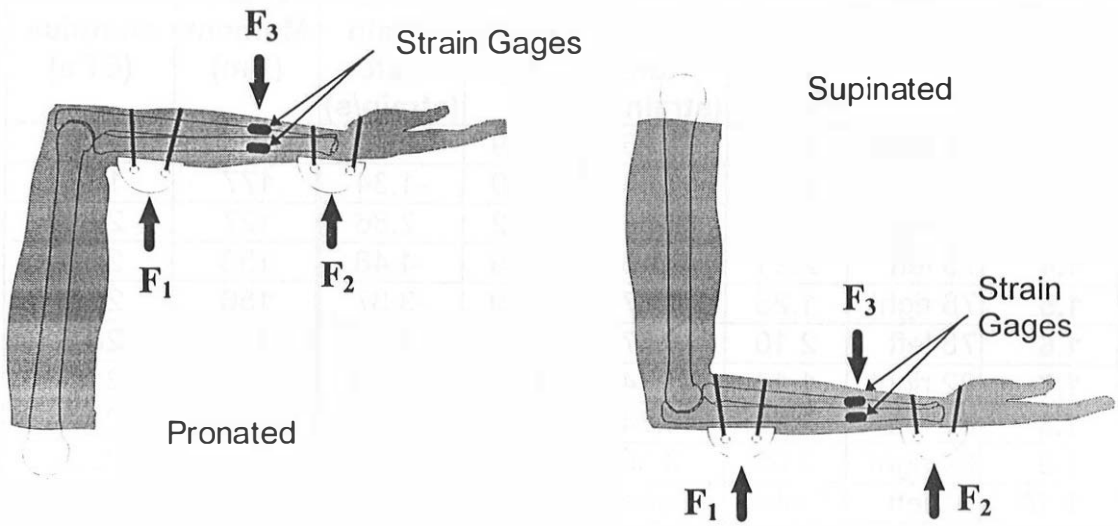

Figure 3: Specimen Preparation for the Pronated and Supinated Forearm Test Configurations.

RESULTS AND DISCUSSION

HUMERUS TESTS – The results from the humerus dynamic three-point drop tests are presented in table 2. The average peak moment of 154 ± 27 Nm can be mass scaled using the technique described by Eppinger *et al.* (1984) to produce the injury tolerance for the 5th% small female humerus of 128 ± 19 Nm. Although this value is very similar to the 134 Nm presented by Kirkish *et al.* (1996), the similarity appears due to two opposing factors. The humeri in the study by Kirkish *et al.* were male and would tend to result in a higher value than female humeri; however, the tolerance was not scaled for dynamic testing, impact velocity of 0.22 m/s versus 3.6. m/s in the present study. Also, the relatively low standard deviation in the present study is a result of the close grouping of the small female sample population.

The average strain rates of 3.70 ± 1.34 strain/second and -3.56 ± 1.36 strain/second for the anterior and posterior gages respectively highlight the dynamic nature of the test and should be similar to humerus strain rates seen during side air bag loading. The strain gage wire was broken during the event in the two tests that are marked as 'failed.' Using simple beam theory and ignoring shear affects, the average dynamic elastic modulus was found to be 24.5 ± 3.9 GPa. This was determined by plotting the stress, taken from the applied moment and cross-sectional bone properties, versus the strain directly measured from the in-situ strain gages. The slope of the linear region for each humerus was recorded and averaged. This dynamic elastic modulus should prove useful for finite element modeling of the humerus.

Table 2: Humerus Dynamic Three-point Drop Test Results

Test Number	Subject Aspect	Ant. Strain (%)	Ant. Strain Rate (strain/s)	Post. Strain (%)	Post. Strain Rate (strain/s)	Peak Moment (Nm)	Elastic Modulus (GPa)
1.1	79 right	1.14	1.26	-1.09	-1.34	167	21.0
1.2	79 left	1.24	1.33	-1.49	-1.34	177	19.7
1.3	75 right	2.21	3.69	-1.22	-2.86	127	29.0
1.4	75 left	2.91	5.48	-1.75	-4.48	153	24.0
1.5	78 right	1.25	3.87	-1.09	-3.37	156	22.2
1.6	78 left	2.10	4.57	-1.72	-5.25	170	28.2
1.7	82 right	1.14	3.74	-1.20	-3.69	113	31.5
1.8	82 left	1.18	4.74	-1.06	-4.15	139	24.3
1.9	81 right	2.65	3.36	-1.17	-4.70	146	21.5
1.10	81 left	Failed	Failed	-1.18	-5.12	134	19.3
1.11	80 right	1.68	4.76	-1.13	-2.88	216	26.5
1.12	80 left	1.06	3.96	Failed	Failed	147	26.3
Average		**1.69**	**3.70**	**-1.28**	**-3.56**	**154**	**24.5**
Std. Dev.		**0.67**	**1.34**	**0.25**	**1.36**	**27**	**3.9**

FOREARM TESTS – Three matched pairs of forearms, tests 2.1 through 2.6, were tested with one forearm supinated and the other pronated to directly compare the differences. The results from all the forearm tests are presented in Tables 3 and 4 separated by test condition. The instance of peak strain is noted as 'time' for all tests. The strain rates were calculated from the linear region before fracture from the strain time history plots. Within the three matched pair tests, the supinated position was significantly stronger ($p = .02$) than the pronated position with a 21% higher average peak moment of 92 ± 5 Nm versus 75 ± 7 Nm respectively. Given this difference and the desire to produce a conservative injury tolerance, tests 2.7 through 2.10 were performed in the pronated position. Also, it is advantageous to choose this position given that typically the forearm is pronated while driving.

Table 3: Supinated Forearm Dynamic Three-point Drop Test Results

		Radius			Ulna				
Test	Subject Aspect	Peak Strain (%)	Time (ms)	Strain Rate (strain/ sec)	Peak Strain (%)	Time (ms)	Strain Rate (strain/ sec)	Peak Moment (Nm)	Time (ms)
2.1	1013 left	1.180	4.7	6.78	.889	5.2	9.94	87	4.9
2.4	84 right	1.170	8.5	4.40	1.175	8.6	4.84	92	8.7
2.5	58 left	1.640	7.1	4.10	.757	7.8	4.30	96	7.5
Average		**1.330**	**6.8**	**5.10**	**.940**	**7.2**	**6.36**	**92**	**7.0**
Std. Dev.		**.270**	**1.9**	**1.50**	**.214**	**1.8**	**3.11**	**5**	**1.9**

Table 4: Pronated Forearm Dynamic Three-point Drop Test Results

		Radius			Ulna				
		Peak Strain	Time	Strain Rate	Peak Strain	Time	Strain Rate	Peak Moment	Time
2.2	1013 right	.775	4.8	4.50	.568	3.0	4.50	69	4.7
2.3	84 left	1.160	11.5	3.24	.525	7.9	1.85	82	11.4
2.6	58 right	1.830	9.2	2.05	.606	4.0	4.74	74	9.2
2.7	66 right	1.240	6.5	4.09	.241	3.7	1.24	48	6.5
2.8	72 right	1.880	8.9	2.54	.156	4.5	1.40	83	9.0
2.9	67 left	.961	5.3	5.62	.393	2.5	3.00	58	5.6
2.10	73 right	1.280	8.5	3.45	.286	4.2	2.17	73	8.6
Average		**1.300**	**7.8**	**3.64**	**.396**	**4.3**	**2.70**	**70**	**7.8**
Std. Dev.		**.380**	**2.2**	**1.12**	**.162**	**1.6**	**1.32**	**13**	**2.2**

The average peak moment for the pronated forearms was 70 ± 13 Nm, and when mass scaled for the 5th% female, the dynamic injury tolerance was determined to be 58 ± 12 Nm. This value agrees reasonably well with the results presented by Bass *et al.* (1997), who determined a forearm injury value of 67 ± 13 Nm as the 50% risk of fracturing one bone in the forearm. This similarity suggests a preliminary validation of the biofidelity of the SAE instrumented upper extremity.

The average radius and ulna strain rates for the pronated tests were 3.64 ± 1.12 and 2.70 ± 1.32 strain/second respectively. The relatively high standard deviation for strain rates may be due to variability in the initial positioning of the strain gages relative to the neutral axis, slight radius and ulna rotation during the impact, and the non-uniform geometry of the radius and ulna between specimens. There was no significant difference in radius and ulna strain rates between the two positions. The strain rates compare well to rates recorded for air bag loading which ranged from 1.3 to 5.3 strain/second. The difference in loading between the pronated and supinated positions was investigated in more detail by examining the impact time histories as well as the forearm fracture patterns and locations.

FOREARM IMPACT TIME HISTORIES – The in-situ strain gages were used to determine not only peak strain and strain rate, but also the fracture times of the radius and ulna. Since the trigger time depends on the amount of soft tissue and trigger strip placement for each test, the time history plots can only be used as a relative measure of fracture time within each test. In the supinated position the average difference in fracture time between the radius and ulna was a negligible 0.4 ± 0.3 ms. However, the pronated tests yielded an average difference in fracture time of 3.6 ± 1.2 ms, with the ulna breaking before the radius in every test. This difference is very significant ($p = .0001$) for comparing only the matched pairs, but just significant ($p = .05$) for all tests. As illustrated in Figures 4 and 5, this trend implies that in the pronated position, the ulna and radius are loaded independently, while in the supinated position the ulna and radius are loaded together as a combined structure. These two figures also highlight the difference in peak strain values between the two positions. While the average radius peak strains for supinated and pronated tests were similar at 6.8 ± 1.9 % and 7.8 ± 2.2 % respectively, the average ulna peak strains were significantly different ($p = .03$) at 7.2 ± 1.8 % for the supinated tests and 4.3 ± 1.6 % for the pronated tests. Furthermore, in pronation the peak strain for the ulna was significantly less ($p = .0007$) than the peak strain in the radius.

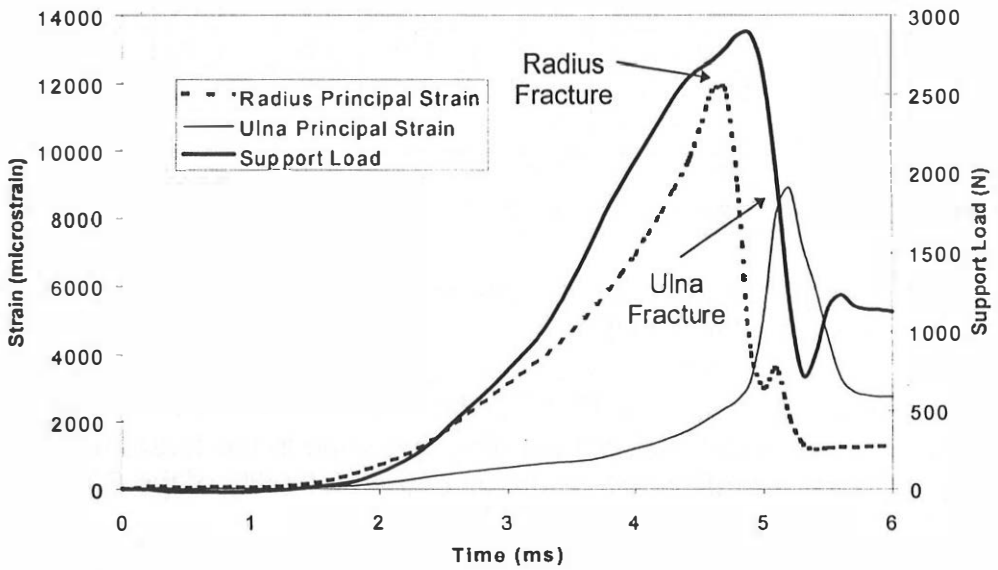

Figure 4: Strain and Support Load Time History for the Supinated Test 2.1

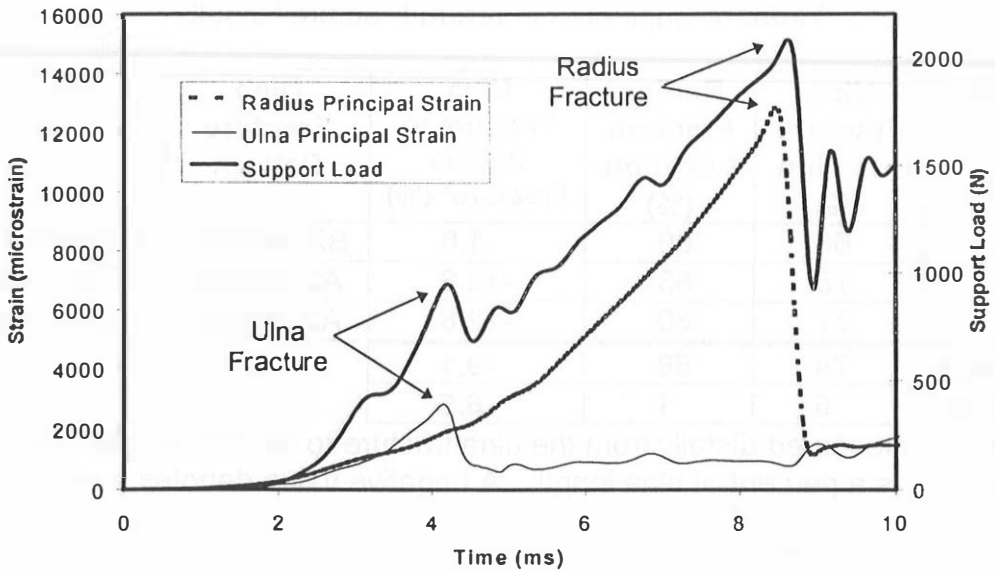

Figure 5: Strain and Support Load Time History for the Pronated Test 2.10

FOREARM FRACTURE ANALYSIS -- The Post-test X-rays were used to assess fracture pattern and location. Measurements were taken to assess relative fracture locations using mid-fracture points. The distance from the olecranon or radial head to the mid-fracture point was expressed as a percentage of the bone's total length. This technique allowed us to compensate for radiographic magnification and compare fracture location. The distance between the radius and ulna fracture was determined and expressed as a percentage of the ulnar length. Table 5 details the supinated tests while Table 6 contains the pronated tests.

The fracture patterns were confirmed with necropsies of each forearm. No evidence of disruption was seen at the proximal and distal radio-ulnar joints. The fracture pattern was documented using the classification system devised by Johner and Wruhs to describe tibial fractures [Johner *et al.*, 1983] This system classifies according to the fracture pattern and the likely fracture mechanism: A1=spiral; A2=oblique; A3=transverse; B1=butterfly fragment by torsion; B2 and B3=butterfly by bending with one or several fragments respectively; C1=comminuted by torsion; C2=segmental; C3=crush. While the majority of the radius fractures in the pronated position were of the B2-butterfly type, no obvious fracture pattern trends were seen.

Table 5: Supinated Forearm Fracture Results

Test	Ulna Fracture Location (%)	Radius Fracture Location (%)	Ulna Fracture to Radius Fracture* (%)	Ulna Fracture Pattern	Radius Fracture Pattern
2.1	68	60	-1.6	B2-butterfly	A3-transverse
2.4	78	58	-12.8	A2-oblique	A3-transverse
2.5	77	60	-12.8	A2-oblique	B2-butterfly
Average	**74**	**59**	**-9.1**		
Std Dev	**6**	**1**	**6.5**		

* Distance measured distally from the ulna fracture to the radius fracture expressed as a percent of ulna length. A negative value denotes a radius fracture that is proximal to the ulna fracture.

Table 6: Pronated Forearm Fracture Results

Test	Ulna Fracture Location (%)	Radius Fracture Location (%)	Ulna Fracture to Radius Fracture (%)	Ulna Fracture Pattern	Radius Fracture Pattern
2.2	66	63	10.7	A2-oblique	A3-transverse
2.3	72	67	0.4	A3-transverse	B2-butterfly
2.6	69	61	-2.7	B2-butterfly	B2-butterfly
2.7	72	63	-9.0	A2-oblique	B2-butterfly
2.8	68	62	1.7	A2-oblique	B2-butterfly
2.9	69	66	3.8	B2-butterfly	B2-butterfly
2.10*	85	68	-11.7	A2-oblique	A2-oblique
Average	**72**	**64**	**-1.0**		
Std Dev	**6**	**3**	**7.6**		

* Previous healed proximal fracture of the radius and ulna, new fracture occurred distal to the old fracture cite

The forearm was impacted at a point that would correspond to a percentage of total ulna length of 66%. In both groups the ulna fracture occurred distal to this point, 74 ± 6% in the supinated position and 72 ± 6% in the pronated position. However, the relationship of ulna fracture to the radius fracture between the supinated and pronated groups was different. In the supinated group the radius fracture occurred proximal to the ulna fracture with an average distance of -9.1 ± 6%, while in the pronated group, the average distance between fractures was -1.0 ± 7.6%. While this difference is not significant ($p = .09$) it does indicate a trend. These results suggest variability in the fracture location depending on whether the forearm is supinated or pronated. This variability is also evident when comparing the average fracture

locations for each bone separately. The radius fracture location was significantly ($p = .003$) more proximal, $59 \pm 1\%$ versus $64 \pm 3\%$, in the supinated group versus the pronated group. Although the ulna fracture location seemed more distal, $74 \pm 6\%$ versus $72 \pm 6\%$, in the pronated group versus supinated group, this comparison was not significant ($p = .52$). These observations were confirmed by direct comparison of the matched pair's X-rays as shown in Figure 6.

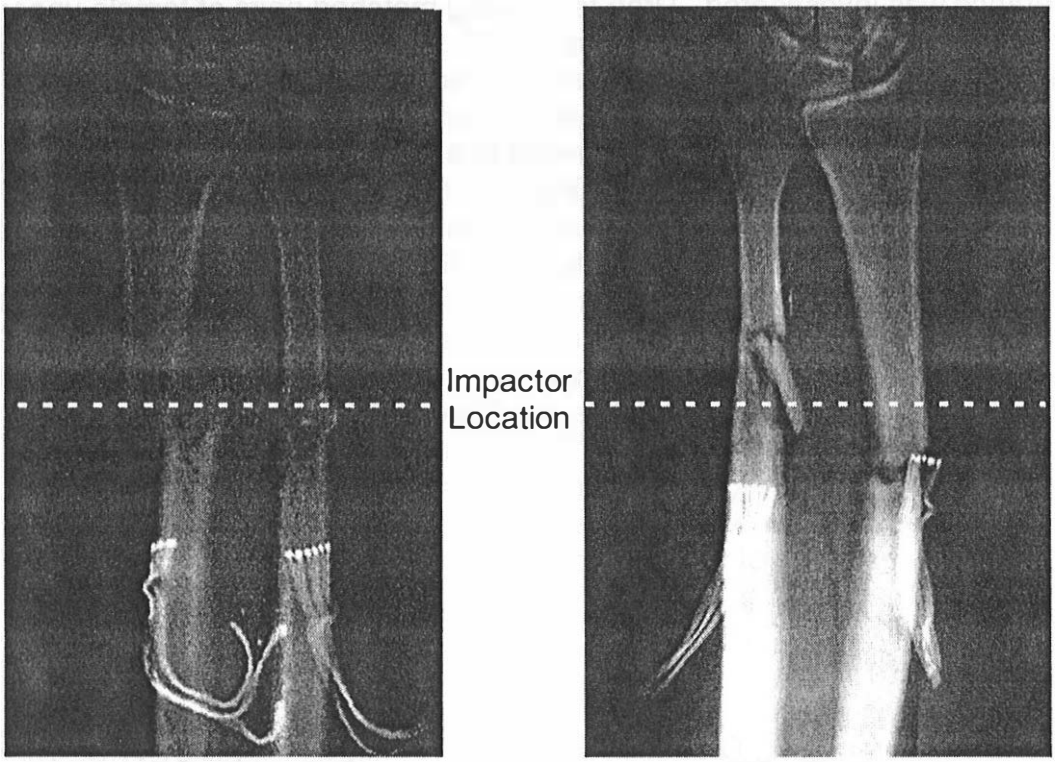

Figure 6: Comparison of the Pronated Fracture Location for Forearm Test 2.3 Versus the Matched Supinated Fracture Location for Test 2.4

These results suggest that the radius and ulna are being loaded sequentially in the pronated arm and the subsequent fractures are occurring directly beneath the impactor head. The ulna is loaded and fails before the radius starts to be significantly loaded. In the supinated position the impact force is more evenly distributed between the two bones. The tendons and muscle bellies of the forearm flexor compartment will also help distribute the impactor load in the supinated position, whereas in the pronated position the ulna is relatively exposed. The difference in fracture location suggests that the supinated forearms are breaking at weaker points rather than directly underneath the impactor as in the pronated forearms.

CONCLUSIONS

The dynamic bending strength of the 5th% female humerus was determined to be 128 Nm with a dynamic elastic modulus of 24.4 GPa. It is anticipated that these values will be utilized for investigations of side air bag loading of the female humerus.

For use with driver-side air bag studies, the female forearm injury tolerance was investigated. Drop tests using matched pairs of female upper extremities revealed that the forearm is 21% stronger in the supinated position. The fracture location for the pronated tests occurred directly under the impactor, while in the supinated tests the radius fractures more proximal and the ulna more distal than in the pronated position. Given that the forearm is typically pronated in the driving position and the desire to produce a conservative injury criterion, the weaker pronated position was used and scaled to give the dynamic bending strength of the 5th% female forearm of 58 Nm.

The similarity between the presented forearm injury criterion of 58 Nm for the female cadaver and that found by Bass et al. of 67 Nm for the SAE upper extremity suggests a preliminary biofidelity validation. The higher dummy response is most likely due to the fact that the SAE upper extremity is slightly more massive than the reference 5th% female. While no discussion of the dummy's kinematic biofidelity is given, it is suggested that the SAE upper extremity tends to over estimate the forearm loads and thus provides a conservative estimate of the injury potential.

REFERENCES

Bass C.R., Duma S.M., Crandall J.R., Morris R., Martin P., Pilkey W.D., Hurwitz S., Khaewpong N., Eppinger R., Sun E., The Interaction of Air Bags With Upper Extremities. SAE Paper 973324, 41st Stapp International Car Crash Conference, 1997.

Carter D.R., Caler W.E., Cycle-dependent and time-dependent bone fracture with repeated loading. Journal of Biomechanical Engineering, 105:166-170, 1983.

Eppinger R.H., Marcus J.H., Morgan R.M., Development of Dummy and Injury Index for NHTSA's Thoracic Side Impact Protection Research Program. SAE Paper 840885, 28th Stapp International Car Crash Conference, 1984.

Johner R., Wruhs O., Classification of Tibial Shaft Fractures and Correlation with Results after Rigid Internal Fixation, Clin. Orthop., 1983. 178, p7-25.

Kallieris D., Rizzetti A., Mattem R., Jost S., Priemer P., Unger M., Response and Vulnerability of the Upper Arm Through Side Air Bag Deployment. SAE Paper 973323, 41st Stapp International Car Crash Conference, 1997.

Kirkish S.L., Begeman P.C., Paravasthu N.S., Proposed Provisional Reference Values for the Humerus for Evaluation of Injury Potential. SAE Paper 962416, 40th Stapp International Car Crash Conference, 1996.

Kuppa S.M., Yeiser C.W., Oslon M.B., Taylor L., Morgan R., Eppinger R., RAID - An Investigation Tool to Study Air Bag/Upper Extremity Interactions. SAE Paper 970399, SAE International Congress and Exposition, 1997.

Messerer O., *Uber Elasticitat und festigkeit der Menschlichen Knocken*, Verkag der J.G. Cotta'schen Buchhandlung, Stuttgard, 1880.

National Highway Traffic Safety Administration, Third Report to Congress: Effectiveness of Occupant Protection Systems and Their Use, U.S. Department of Transportation, December 1996.

Weber C., *Chirurgishe Erfahrungen and Untersuchungen*, Berlin, 1859.

APPENDIX

Table A1: Specimen Information for Female Humerus Tests

Test	Aspect	Age (years)	Body Mass (kg)	Cause of Death
1.1	79 right	54	71.1	Myocardial Infraction
1.2	79 left	54	71.1	Myocardial Infraction
1.3	75 right	59	64.4	Congestive heart failure
1.4	75 left	59	64.4	Congestive heart failure
1.5	78 right	41	56.0	Ovarian carcinoma
1.6	78 left	41	56.0	Ovarian carcinoma
1.7	82 right	50	49.1	Breast and liver carcinoma
1.8	82 left	50	49.1	Breast and liver carcinoma
1.9	81 right	74	52.7	Breast carcinoma
1.10	81 left	74	52.7	Breast carcinoma
1.11	80 right	66	59.0	Lung carcinoma
1.12	80 left	66	59.0	Lung carcinoma

Table A2: Specimen Information for Female Forearm Tests

Test	Aspect	Age (years)	Body Mass (kg)	Cause of Death
2.1	1013 left	64	49.9	Lung Cancer
2.2	1013 right	64	49.9	Lung Cancer
2.3	84 left	59	80.0	Adenocarcinoma of the lung
2.4	84 right	59	80.0	Adenocarcinoma of the lung
2.5	58 left	61	52.1	Bronchial carcinoma
2.6	58 right	61	52.1	Bronchial carcinoma
2.7	66 right	67	61.0	Respiratory failure
2.8	72 right	51	55.8	Ventricular failure
2.9	67 left	67	52.6	Respiratory failure
2.10	73 right	61	57.2	Myocardial infraction